Mangrove forest changes detection and biocapacity estimation from 1985 to 2018 in China

Zheng Yuhan*, and Wataru Takeuchi
Institute of Industrial Science, the University of Tokyo, Japan

Abstract: Mangroves in China have experienced various changes in different time periods due to anthropogenic disturbances, climate change and national restoration policy. However, few studies quantitatively analyzed these changes. This study detected the changes of mangroves in China from 1985 to 2018 by combing Landsat and ALOS PALSAR images. The results demonstrated that the total areas of China's mangrove in 1985, 1996, 2007, 2010 and 2018 were 20,086 ha, 18,033 ha, 22,428 ha, 23,639 ha and 24,602 ha respectively. Mangrove area began to increase after 1990s mainly due to the national conservation actions. The causes for mangrove changes are various in different regions and time periods. However, most mangroves gained from aquaculture and lost to built-up. The changes between mangroves and other land covers also caused the biocapacity changes in coastal zone which contributed to around 17,000 gha increase of biocapacity from 1996 to 2018.

1 Introduction

Fig. 1 In situ photos of mangroves in Zhejiang province, China.

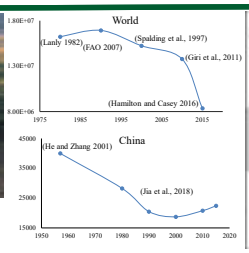

Fig. 2 Mangrove area changes.

Fig. 3 Location of study area

Objectives:

- Quantify the long-term mangrove dynamics with high accuracy by combining Landsat and ALOS PALSAR images and analyze the main driving force for each province;
- Estimate the biocapacity changes in coastal ecosystems caused by the conversion between mangrove and other land covers.

2 Methodology

2.1 Mangrove mapping and change detection

2.2 Biocapacity estimation

Calculation of biocapacity for Single Land Use Type:

$$BC = A \times YF \times IYF \times EQF$$ *(National Footprint Accounting, 2019)*

BC: biocapacity of a given land use type, gha (global hectare)
A: Area of a given land use type within a country, nha-1
YF: Yield factor of a given land use type within a country, wha nha-1
IYF: Intertemporal Yield factor of a given land use type for that year
EQF: Equivalence factor for given land use type, gha wha-1

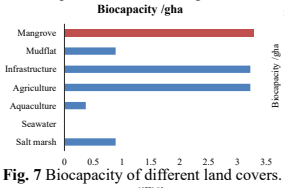

Fig. 7 Biocapacity of different land covers.

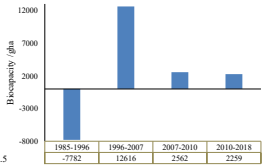

Fig. 8 Biocapacity changes in different time periods.

3 Results

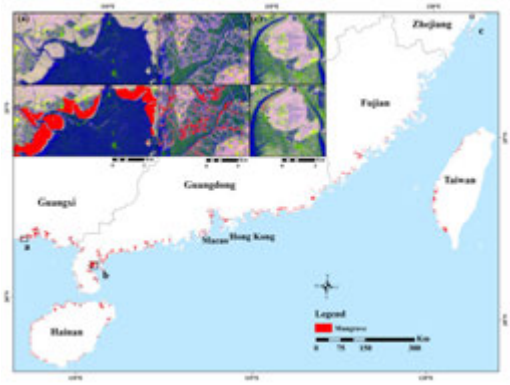

Fig. 4 Spatial distribution of China's mangroves in 2018 and zoom views of three mangrove natural reserves. The background of (a)-(c) are ALOS PALSAR-2 mosaic in 2018 shown in R: G: B = HH: HV: HH-HV composite.

Table 1. Classification accuracy.

Province	Area (ha)	Overall accuracy (%)	Kappa coefficient
ZJ	24.48	88.89	0.6200
FJ	908.55	98.76	0.9496
GD	9,214.63	96.22	0.9042
GX	9,095.71	98.30	0.9571
HN	4,269.78	93.25	0.8646
HK	533.34	99.02	0.9794
Macao	10.62	-	-
TW	542.34	93.83	0.8115
Total	24,602.45	96.03	0.8858

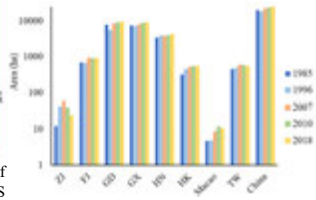

Fig. 5 Mangrove area changes in China.

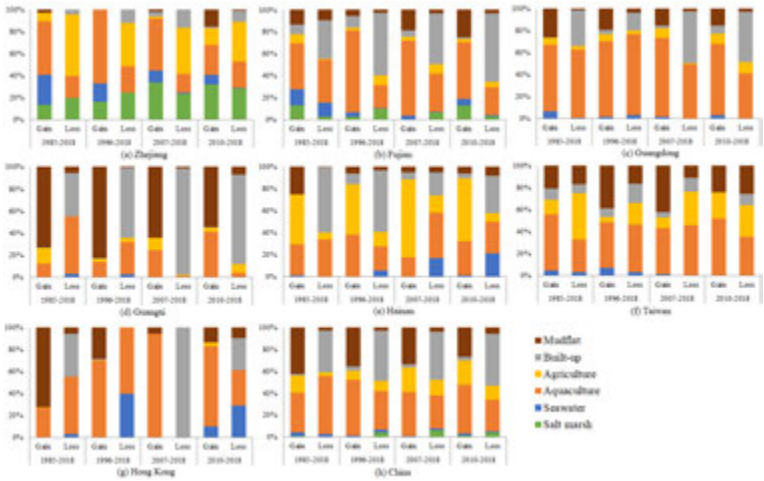

Fig. 6 Mangrove gain and loss in terms of different land cover.

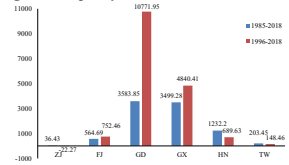

Fig. 9 Biocapacity changes in different regions.

Biocapacity :
The area changes of mangroves contribute to the increase of biocapacity in China:
17,437 gha (from 1996 to 2018)
4,821 gha (from 2007 to 2018)
2,259 gha (from 1996 to 2018)

4 Conclusions

- Mangroves area decreased from 1985 to 1996, while kept increasing after 1996 mainly due to the national conservation actions since 1990s.
- Most mangrove gains came from aquaculture and mudflat, while losses were due to built-up and aquaculture.
- Biocapacity changes are not only related to mangrove area changes but also the change types.
- The uncertainties: Training samples (1985, 1996); Indices selected for classification; Tidal inundation; Different mangrove species and ages.

For references and details, contact: Zheng Yuhan, Bw-601, 6-1, Komaba 4-chome, Meguro, Tokyo 153-8505 JAPAN (URL:http://wtlab.iis.u-tokyo.ac.jp/E-mail: yuhan@g.ecc.u-tokyo.ac.jp)